Pharmacogenetic variability and the probability of site of action target attainment during tuberculosis meningitis treatment: a physiologically based pharmacokinetic modeling and simulations study

Mehta, K.M.; Narayanan, N.; Heysell, S.K.; Bisson, G.P.; Subbian, S.; Kurepina, N.; ... ; Vinnard, C.

Tuberculosis 137 (2022) 102271

Contents lists available at ScienceDirect

Tuberculosis

journal homepage: www.elsevier.com/locate/tube

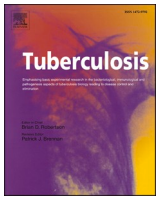

Pharmacogenetic variability and the probability of site of action target attainment during tuberculosis meningitis treatment: A physiologically based pharmacokinetic modeling and simulations study

Krina Mehta [a,*], Navaneeth Narayanan [b], Scott K. Heysell [c], Gregory P. Bisson [d], Selvakumar Subbian [e], Natalia Kurepina [f], Barry N. Kreiswirth [f], Christopher Vinnard [g,1]

[a] Leiden University, Leiden, the Netherlands
[b] Rutgers University, Ernest Mario School of Pharmacy, Piscataway, NJ, USA
[c] University of Virginia, Division of Infectious Diseases and International Health, Charlottesville, VA, USA
[d] University of Pennsylvania, Perelman School of Medicine, Philadelphia, PA, USA
[e] Public Health Research Institute, New Jersey Medical School, Newark, NJ, USA
[f] Center for Discovery & Innovation, Hackensack Meridian Health, Nutley, NJ, USA
[g] Rutgers University, New Jersey Medical School, Newark, NJ, USA

A B S T R A C T

Objective and methods: Our objective was to investigate the role of patient pharmacogenetic variability in determining site of action target attainment during tuberculous meningitis (TBM) treatment. Rifampin and isoniazid PBPK model that included SLCO1B1 and NAT2 effects on exposures respectively were obtained from literature, modified, and validated using available cerebrospinal-fluid (CSF) concentrations. Population simulations of isoniazid and rifampin concentrations in brain interstitial fluid and probability of target attainment according to genotypes and *M. tuberculosis* MIC levels, under standard and intensified dosing, were conducted.
Results: The rifampin and isoniazid model predicted steady-state drug concentration within brain interstitial fluid matched with the observed CSF concentrations. At MIC level of 0.25 mg/L, 57% and 23% of the patients with wild type and heterozygous SLCO1B1 genotype respectively attained the target in CNS with rifampin standard dosing, improving to 98% and 91% respectively with 35 mg/kg dosing. At MIC level of 0.25 mg/L, 33% of fast acetylators attained the target in CNS with isoniazid standard dosing, improving to 90% with 7.5 mg/kg dosing.
Conclusion: In this study, the combined effects of pharmacogenetic and *M. tuberculosis* MIC variability were potent determinants of target attainment in CNS. The potential for genotype-guided dosing during TBM treatment should be further explored in prospective clinical studies.

1. Introduction

Central nervous system infection is the most severe manifestation of TB, with approximately one-half of affected patients suffering severe neurologic disability or death [1,2]. In the absence of known or suspected drug-resistant disease, TB treatment guidelines recommend standard dosing of isoniazid and rifampin as part of the first-line regimen [3]. Clinical trials of intensified dosing of rifampin for tuberculosis meningitis (TBM) have yielded mixed results [4–6], perhaps owing to differences in the dosing regimen of the intensified arm [7]. There still remains considerable uncertainty regarding the optimal initial treatment of TBM patients [6].

For the treating clinician, limited information is available to guide the selection of a drug regimen for a TBM patient. The susceptibility of *M. tuberculosis* to a given anti-TB drug is typically established with phenotypic resistance testing at a "breakpoint" MIC, with a delay of several weeks after cultures are obtained [8]. While these breakpoint MIC values have been interrogated in the treatment of pulmonary TB [9], the relationship between MIC breakpoint and clinical response in the treatment of TBM patients is less examined [2]. Furthermore, there is an emerging understanding of the contribution of host genetics to the pharmacokinetic (PK) variability of both isoniazid and rifampin [10]. For isoniazid, this source of variability is primarily driven by the metabolizing enzyme responsible for isoniazid elimination, the N-acetyltransferase-2 (NAT2) gene [11]. More recently, pharmacogenetic variability in the hepatic OATP1B1 uptake transporter gene (SLCO1B1) has been identified as a driver of rifampin PK variability, as individuals who possessed the variant allele demonstrated increased rifampin

* Corresponding author.
E-mail address: k.m.mehta@lacdr.leidenuniv.nl (K. Mehta).
[1] Current employer GlaxoSmithKline plc,

https://doi.org/10.1016/j.tube.2022.102271
Received 7 April 2022; Received in revised form 1 September 2022; Accepted 12 October 2022
Available online 20 October 2022

clearance compared to individuals with the homozygous wild-type gene [12,13].

For both isoniazid and rifampin, the pharmacodynamic effect is based on achieving PK exposure at the site of infection, defined by the area under the concentration-versus-time profile (AUC), that is sufficiently greater than the MIC of the infecting *M. tuberculosis* strain [14,15]. Prior work has examined the impact of phenotypic drug resistance on the clinical outcomes of TBM, demonstrating that initial isoniazid and/or rifampin resistance is associated with death before treatment completion [16,17]. We sought to extend this work by examining the likelihood of target attainment among TBM patients with putative drug-susceptible disease, as defined by MIC levels for isoniazid and rifampin below the CLSI breakpoint [18]. We hypothesized that sub-breakpoint MIC levels would correspond to unattainable targets among TBM patients with genotypes of SLCO1B1 (for rifampin) or NAT2 (for isoniazid) that correspond with lower systemic exposures.

2. Methods

2.1. Rifampin and isoniazid PBPK modeling with genotype effects of SLCO1B1 and NAT2

A previously developed rifampin whole-body PBPK model was used as the base model [19]. The rifampin PBPK model included metabolism by enzyme arylacetamide deacetylase (AADAC), transport by organic anion-transporting polypeptide transporter (OATP1B1) and P-glycoprotein, along with the auto-induction of AADAC, OATP1B1, P-glycoprotein, and CYP3A4. Partition-coefficients from plasma to various tissues, including brain interstitial and intracellular compartments, were calculated based on Rodgers and Rowland method [20]. The model included efflux transporter, P- glycoprotein, mediated passive transport through blood-brain barrier [19]. The model also included the effect of hepatic OATP1B1 (encoded by the gene SLCO1B1) on rifampin clearance (Supplementary Materials 1).

To quantify the effects of SLCO1B1 pharmacogenetic variability on rifampin exposure, we first reviewed the available literature. A clinical study that included rifampin PK and SLCO1B1 genotypes identified an association of SLCO1B1 SNP c.463CC (rs11045819 wild type) or c.463CA (rs11045819 heterozygous) with plasma concentrations of rifampin in TB patients (n = 72 pulmonary TB patients from Africa, North America, and Spain) [13]. We performed a comparison of this SNP with data collected in a prospective cohort study of 40 HIV/TB patients in Botswana and also identified an association between SLCO1B1 rs11045819 and rifampin exposure [12]. As such, only SLCO1B1 rs11045819 heterozygous vs. wild type categories were selected for evaluations in our PBPK study. The rifampin PBPK model was calibrated using data from literature [13] and the proportional effect of heterozygous category on the maximum transport rate ($Vmax_{OATP1B1}$) was estimated, with all other parameters kept unchanged from the original model. Next, we performed an external validation of the expanded rifampin PBPK model using the PK data from our Botswana study [12]. Patients in the validation dataset were categorized into heterozygous or wild-type groups based on the rs11045819 SNP (Supplementary Materials 2). We validated this expanded rifampin PBPK model by overlaying the model-predicted rifampin concentrations, stratified by SLCO1B1 genotype, with the observed PK data for both genotype categories. Once validated, we performed a sensitivity analysis of the expanded rifampin PBPK model. The sensitivity of the estimates in exposure metrics, including the AUC, C_{max}, and half-life were examined, after introducing 10% variation in absorption and clearance parameters.

We utilized a previously published and validated whole-body PBPK model of isoniazid to simulate PK profiles in CNS compartments during TB treatment [21]. This model incorporated a complex metabolic network, including metabolism of isoniazid by N-acylethanolamine--hydrolyzing acid amidase (NAAA) and NAT2 enzymes, along with further metabolism and transport of the metabolites by various processes. Partition-coefficients from plasma to various tissues, including brain interstitial and intracellular compartments, were calculated based on PK-Sim standard method as incorporated in the software [22].

Additional external validation of the rifampin and isoniazid for the purpose of our analysis was performed by comparing brain interstitial drug predictions against observed drug concentrations measured in cerebrospinal fluid (CSF) collected from TB patients who received various doses of rifampin and isoniazid [5,23,24]. Upon completion of the external validations, the rifampin and isoniazid PBPK model, which included SLCO1B1 and NAT2 covariate effects on drug exposures, respectively, were used for simulations and CNS target attainment evaluations.

2.2. Model codes

The isoniazid PBPK model was unchanged from the previously published version [21] and is available at the GitHub repository https://github.com/HenrikCordes/isoniazid-PBPK-model. The updated rifampin PBPK model with SLCO1B1 genotype effect is available at the GitHub repository https://github.com/krinaj/RIF-INH-PBPK-Models. Additional details about the isoniazid and rifampin PBPK model development, validation, and parameter estimates are available in literature [19,20].

2.3. Observed MIC distributions in M. tuberculosis isolates cultured from CSF in TBM patients

To understand the potential benefit of intensified dosing regimens at the population level, we directly measured the rifampin and isoniazid MIC levels in collection of *M. tuberculosis* isolates that had been obtained from TBM patients in the U.S. state of New Jersey over a 12-year period. In support of statewide molecular epidemiology efforts, the Kreiswirth laboratory routinely performs DNA fingerprinting on all *M. tuberculosis* isolates across the state of New Jersey, recording the anatomic site of culture for each of isolate in the collection [25]. Among those *M. tuberculosis* isolates that had been cultured from CSF and previously determined to be susceptible to both rifampin and isoniazid (n = 34), we determined the MIC for rifampin and isoniazid by agar diffusion [26].

2.4. Target attainment under standard and intensified dosing schemes of isoniazid and rifampin

Isoniazid and rifampin concentrations in venous blood plasma and brain interstitial fluids were simulated using PBPK models. The simulated population contained 1000 virtual adult TBM patients with body weight sampled from prior distribution of body weight from TB patients [12]. Additionally, other physiological and anatomical parameters were varied as described previously to generate the virtual population [21]. Next, we performed separate simulations (n = 1000) for each NAT2 (slow, intermediate, and fast acetylators) and SLCO1B1 (wild-type and heterozygous) genotype [27]. Under each dosing scheme (standard or intensified), the isoniazid or rifampin $AUC_{0\text{-}24}$ following the 10th dose was calculated for brain interstitial fluid compartment.

Next, we calculated the $AUC_{0\text{-}24}$/MIC ratio corresponding to each MIC value for the infecting *M. tuberculosis* strain. Since all MIC values were falling below the breakpoint that defines drug susceptibility or resistance, we also calculated target attainment at higher MIC referring to drug-resistant strains [23]. For each MIC value, we estimated probabilities of target attainment in brain interstitial fluid for both drugs, under standard and intensified dosing strategies. For rifampin, the target was defined as an $AUC_{0\text{-}24}$/MIC ratio of 30, corresponding to a 1 $\log_{10}$ CFU/mL decrease in *M. tuberculosis* bacterial load [28]. Based on the same criteria, the isoniazid target was defined as an $AUC_{0\text{-}24}$/MIC ratio of 43.5 [14]. We selected intensified dosing strategies based on published clinical trial experiences [23,24,29]. Additionally, based on

observed MIC distributions at the population level, cumulative fraction of response under standard and intensified dosing strategies was estimated by sampling from observed distribution of MIC values in CSF of TB patients.

2.5. Software

Physiologically-based PK modeling and simulation was performed in PK-Sim® and Mobi® (Open Systems Pharmacology Suite, v8.0, www.open-systems-pharmacology.org). Statistical analysis and plots were generated in R (R for Windows, v4.1, https://www.r-project.org/) using RStudio (RStudio, v1-554, www.rstudio.com/).

3. Results

3.1. Extension of rifampin PBPK model with SLCO1B1 genotype effects

The rifampin and isoniazid PBPK models included all major contributing factors affecting systemic and CNS exposures, including, protein binding, active and passive transports into various tissues, and relevant metabolism networks. As such, these models were selected for the purpose of our analysis. The updated rifampin PBPK model described observed plasma concentrations for both patients with both wild type and heterozygous SLCO1B1 genotypes (Fig. 1a). The model suggested a 3% proportional increase in OATP1B1 V_{max} among heterozygous genotype patients, compared to wild-type genotype patients (OATP1B1 V_{max} WT = 0.37 μmol/L/min vs. OATP1B1 V_{max} WT = 0.39 μmol/L/min) [13]. All other parameters, other than OATP1B1 V_{max}, remained unchanged from the literature-based model [19]. In an external validation exercise, the simulated plasma concentration-time profile agreed well with observed rifampin PK data (R^2 = 0.96 and 0.93, respectively, p-value<0.0001) for both SLCO1B1 genotypes (Fig. 1b). With a 10% change in parameter estimates, the sensitivity for key rifampin PK parameters was low (between −1 and 1), which further supported the reliability of the rifampin expanded PBPK model.

3.2. Model-predicted isoniazid and rifampin exposures in CNS, stratified by genotype

The rifampin and isoniazid PBPK models predicted steady-state drug concentration within brain interstitial compartment matched well with observed CSF drug concentrations (Fig. 2, Fig. 4). With the standard rifampin dose of 10 mg/kg orally once daily, the mean $AUC_{0\text{-}24}$ ratio for brain interstitial fluid: plasma was predicted to be approximately 0.36 and 0.24 for wild-type and heterozygous groups, respectively. For the standard isoniazid dose (5 mg/kg), the mean $AUC_{0\text{-}24}$ ratio for brain interstitial fluid: plasma was predicted to be approximately 0.76 for fast acetylators and 0.78 for both intermediate and slow acetylators.

3.3. Probability of target attainment in CNS under standard and intensified treatments

Distribution of MIC levels for rifampin and isoniazid in a collection of *M. tuberculosis* isolates that had been cultured from the CSF of patients is presented in Fig. 3. With standard and intensified rifampin dosing, the probabilities of successful rifampin target attainment in brain interstitial

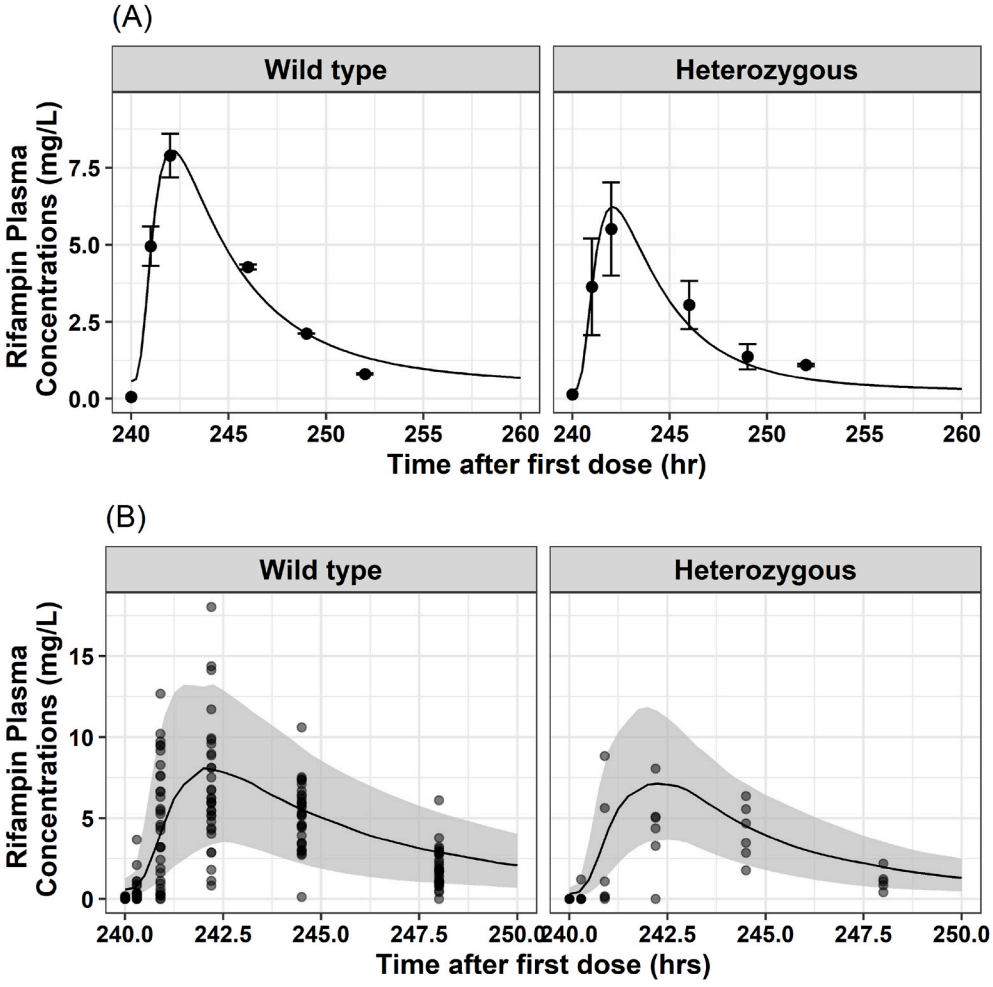

Fig. 1. Development and validation of an expanded rifampin PBPK model to include SLCO1B1 genotype. **(A)** Development of the model to include SLCO1B1 covariate effects (n = 72 patients from Weiner et al., 2010 [**13**]). **(B)** Validation of the expanded rifampin PBPK model (n = 40 patients from Vinnard et al., 2017 [**12**]. Rifampin PBPK model described plasma concentrations time profiles for both SLCO1B1 wild type and heterozygous groups well. Black points with error bars represent mean and SD of observed data, black points represent individual concentrations data, black line represent median of predicted, and grey shading represent 95% confidence interval of the predictions.

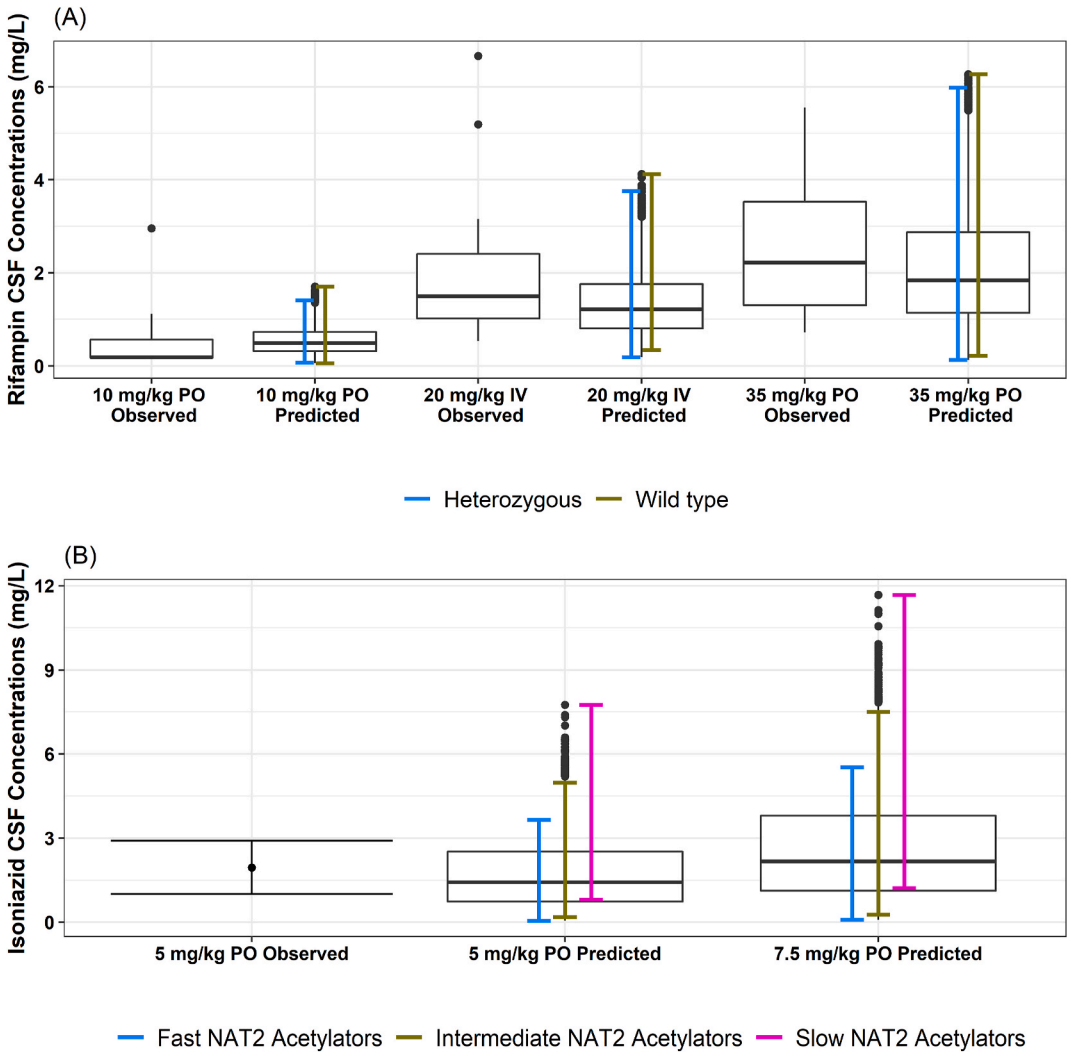

Fig. 2. Validation of the rifampin and isoniazid PBPK models for predictions of drug exposures in the CSF. The PBPK models predicted rifampin and isoniazid steady-state concentrations in brain interstitial compartment matched well with the observed concentrations data from CSF of TB patients [**23**,**24**].

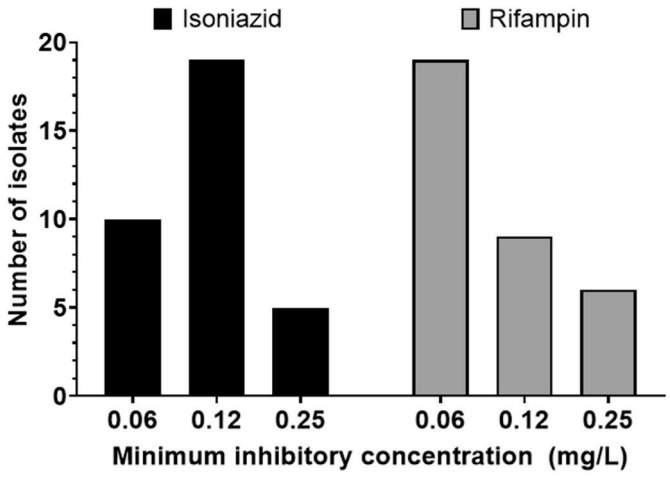

Fig. 3. Distribution of minimum inhibitory concentration levels of isoniazid and rifampin among *M. tuberculosis* isolates that were cultured from CSF in New Jersey over a 12 -year period.

fluid are shown in Fig. 5A. At rifampin MIC level of 0.125 mg/L, 92% of patients with wild-type SLCO1B1 genotype attained the rifampin target in brain interstitial fluid, compared with 86% of the patients with heterozygous SLCO1B1 genotype. At a rifampin MIC level of 1 mg/L, none of the patients with either SLCO1B1 genotype were predicted to achieve rifampin target in brain interstitial fluid. With intensified rifampin dosing of 35 mg/kg and MIC level of 1 mg/L, 42% and 21% of patients with wild-type and heterozygous SLCO1B1 genotype, respectively, attained the rifampin target in brain interstitial fluid. With standard and intensified rifampin dosing, the probabilities of successful isoniazid target attainment in brain interstitial fluid are shown in Fig. 5B. At an isoniazid MIC level that is less than or equal to 0.125 mg/L, nearly all TBM patients regardless of NAT2 genotypes attained the target in brain interstitial fluid at the standard dosing. At an isoniazid MIC level of 1 mg/L, none of the fast or intermediate acetylators and only 12% of slow acetylator patients attained the target in brain interstitial fluid at the standard dosing. At the same MIC, intensified dosing predicted to provide target attainment in none of the fast acetylators, 2% of intermediate acetylators, and 68% of slow acetylators.

Based on observed MIC distributions at the population level (Fig. 3), cumulative fraction of response under standard and intensified dosing strategies was estimated by sampling MIC values from observed distribution of MIC values in CSF of TB patients to calculate target attainment probabilities (Fig. 3). For the drug-susceptible strains, there was 86%

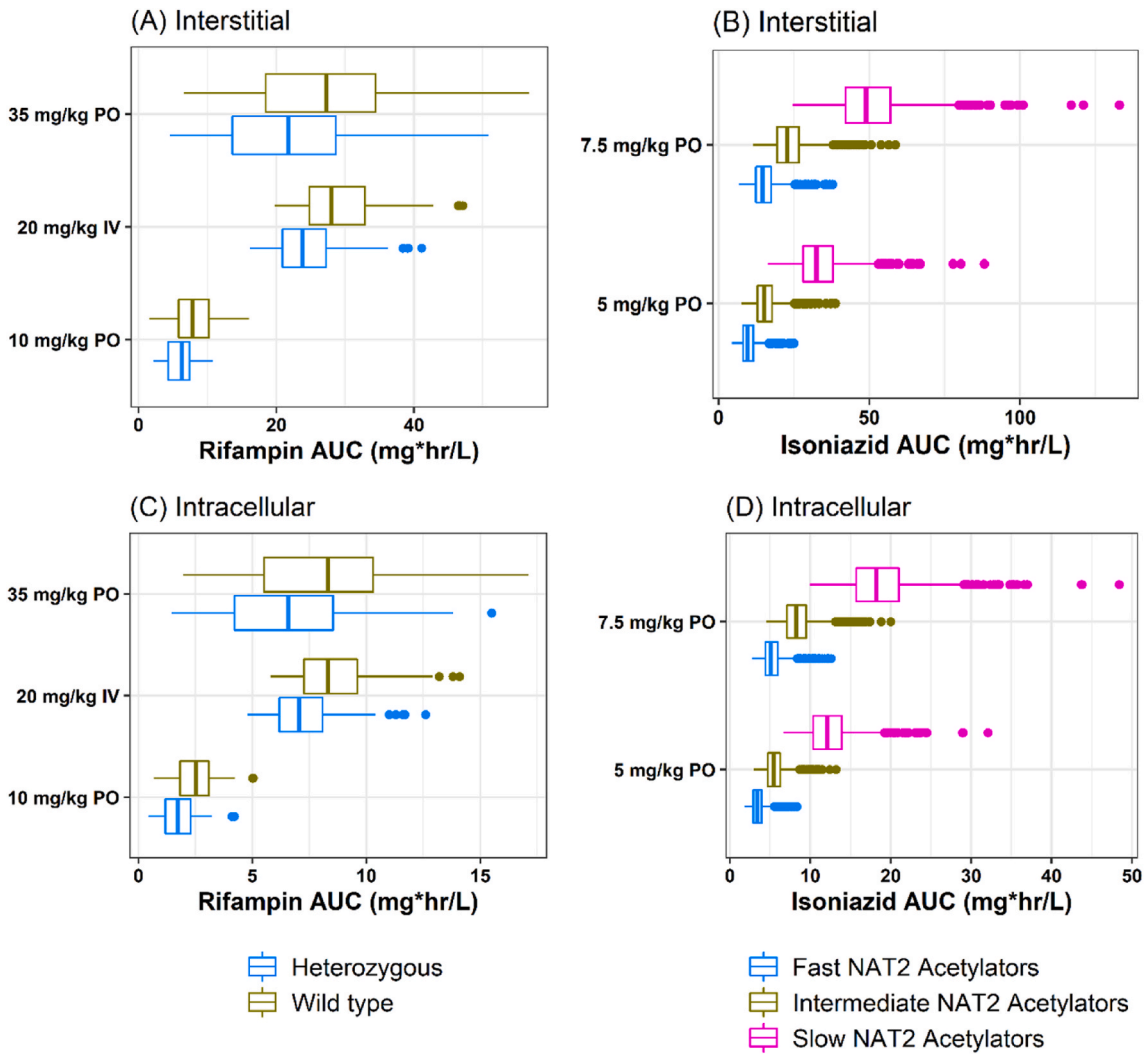

Fig. 4. Predicted steady state rifampin and isoniazid $AUC_{0\text{-}24}$ (mg·hr/L) in the CNS compartments stratified by dosing regimen and genotype. (A) rifampin brain interstitial, (B) isoniazid brain interstitial, (C) rifampin brain intracellular, (D) rifampin brain interstitial. All dosing regimens were administered once daily.

and 99% overall probability of PD target attainment in brain interstitial fluid with standard dosing and intensified dosing of rifampin, respectively. Similarly, for the drug-susceptible strains, there was a 92% and 99% overall probability of target attainment in brain interstitial fluid with standard dosing and intensified dosing of isoniazid, respectively.

4. Discussion

Our objective was to evaluate the probability of target attainment in the CNS during TBM treatment with a first-line regimen that includes isoniazid and rifampin. We used a PBPK modeling approach to incorporate two independent sources of variability: host pharmacogenetics and pathogen MIC levels. Using this approach, we tested the hypothesis that sub-breakpoint MIC levels for isoniazid and rifampin would correspond to essentially unattainable targets among patients with fast elimination genotypes. While our findings support this hypothesis, they also demonstrate that the clinical benefit of intensified dosing regimens are concentrated at certain MIC levels for the infecting *M. tuberculosis* strain.

Adequate PK exposures of anti-TB drugs in the CNS are crucial for treatment success for TBM patients [30]. Current bioanalytical sampling methods do not allow measurements of drug exposure from various CNS sites of TB lesions, such as brain intracellular tuberculomas, and CSF drug concentrations may be used as a summary measure of CNS drug exposure [31]. The whole-body PBPK model that was used in this analysis includes blood cells, plasma, interstitial space, and tissue space for each organ/compartment; drug partitioning into these spaces is based on physicochemical parameters of the drug and physiological parameters of the species. Furthermore, the rifampin PBPK model also includes P-glycoprotein transporter effects at the blood-brain barrier [19]. As such, our PBPK model-based approach in this analysis is useful to predict anti-TB drug target attainment at CNS sites of action in TBM patients, and advances prior understandings based on CSF concentration-time profiles [32–34].

In clinical trials of pulmonary TB patients, intensified dosing of rifampin (up to 50 mg/kg oral) led to fast sterilization activity increasing toxicity [23,29,35]. In TBM patient populations, clinical trials of intensified rifampin dosing have shown mixed results. Rifampin doses up to 15 mg/kg did not show improved survival in a study conducted in Vietnamese patients (n = 817) [4]. In contrast, a clinical trial of intensified rifampin dosing among Indonesian TBM patients (n = 122) led to improvements in mortality without an increased rate of adverse events, with dose increases up to 30 mg/kg [5]. A model-based meta-analysis has found that even doses beyond 30 mg/kg may be expected to improve clinical response [33]. Our work also suggests that unmeasured MIC variability may be a major driver of clinical response, with an additional contribution of SLCO1B1 pharmacogenetic variability in some populations. Importantly, the MIC variability in the current study was

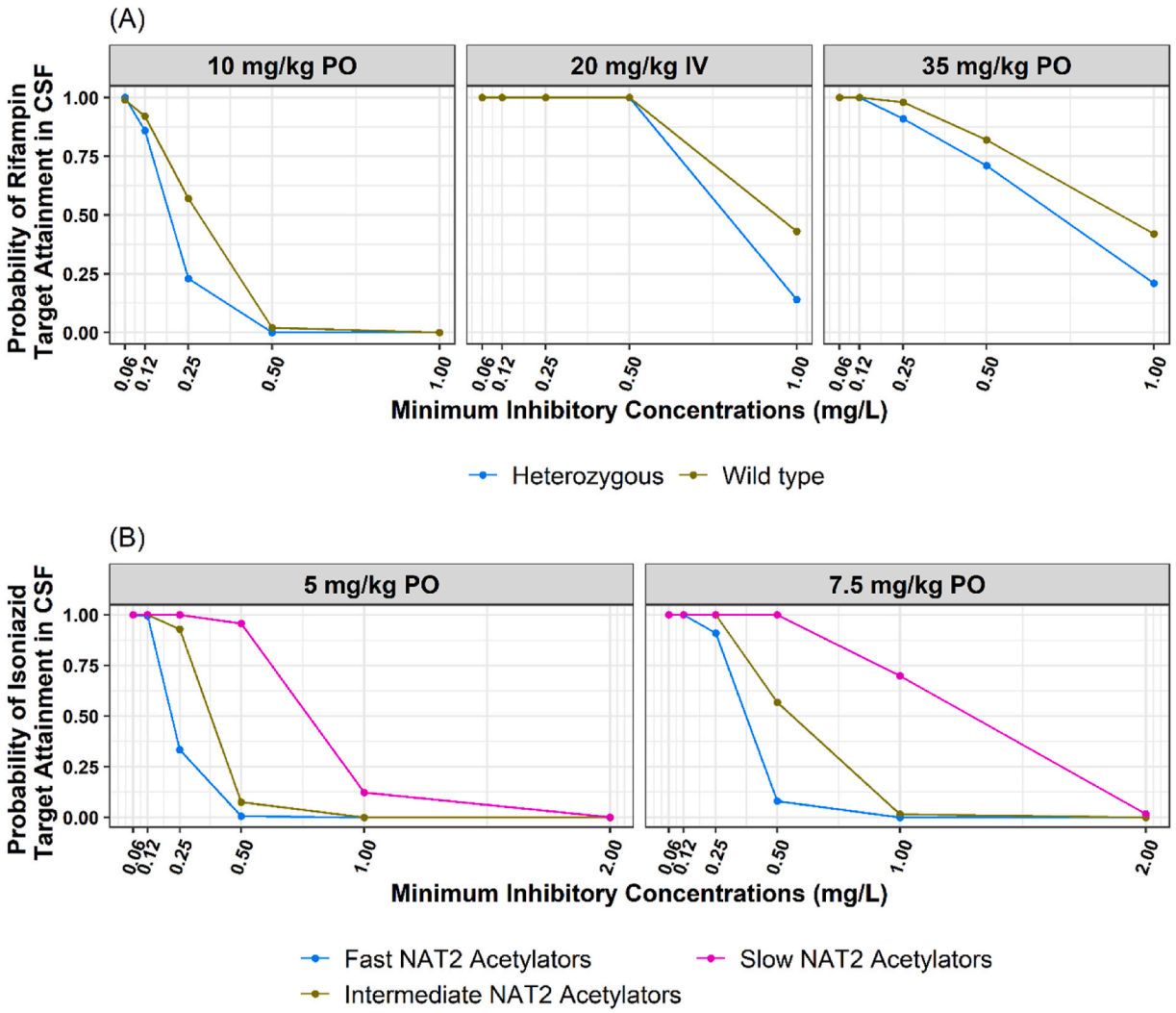

Fig. 5. Target attainment probabilities in brain interstitial compartment under standard and intensified dosing regimens for rifampin and isoniazid stratified by SLCO1B1 and NAT2 genotypes, respectively. All dosing regimen assumed once daily therapy.

entirely sub-breakpoint, meaning that these isolates would be classified as drug-susceptible by the clinical laboratory. With the PBPK model-based simulations, we were able to demonstrate that standard dosing would achieve markedly low probabilities for target attainment for drug-resistant strains by setting MIC to higher values. We propose that future prospective clinical trials of TBM treatment regimens prioritize the capacity for secondary analyses based on these additional sources of variability.

As patient genotyping methods advance to reach a greater number of bedsides in geographic areas with a high burden of TB disease, the potential tradeoffs between personalized medicine and standardized treatment regimens will require greater consideration, regarding incremental benefits and resource utilization. Much attention has been focused on the support of clinical decision-making provided by DNA sequencing of *M. tuberculosis* strains, for example to identify mutants likely to confer phenotypic drug resistance [36]. Yet parallel efforts are underway to identify the patient's genotypic determinants of TB treatment response, including the use of the *LTA4H* genotype to select patients for adjunctive corticosteroid treatment [37], currently studied in a prospective clinical trial [38]. Our findings suggest that these patient genotyping efforts should be expanded to evaluate prospectively the impact of SNPs related to NAT2 and/or SLCO1B1 activity during TBM treatment. This information could be combined with *M. tuberculosis* mutational analysis to identify those patients most likely to benefit from intensified drug therapy, and perhaps to guide further the selection of the intensified dose in the regimen.

A key finding of the current work was the difference in drug exposures between brain interstitial fluid and brain intracellular. According to one model of TBM pathogenesis, the early bloodstream dissemination of *M. tuberculosis* may lead to foci of infection established in the meninges and brain parenchyma, following a vascular distribution [39]. As these tubercles enlarge, there is potential for rupture into the sub-arachnoid space, leading to the signs and symptoms of meningitis, most commonly in a basilar distribution [40]. Yet the tubercles themselves are found in the brain or meningeal tissue, and enlargement without rupture leads to the formation of tuberculomas, which may become clinically apparent as space-occupying lesions. Delayed sterilization of deep CNS anatomic sites during TB treatment, as a consequence of sub-optimal PK exposures, could contribute to the observed risk of paradoxical reaction during TBM treatment [41]. The current PBPK model calculated brain interstitial to intracellular partition coefficients based on standard PBPK modeling methods [42]. As such, the model may not contain all relevant mechanistic details pertaining drug penetration in the brain intracellular compartment. Although further work may be needed to implement all relevant mechanisms of brain intracellular penetration for anti-tuberculosis drugs, our relatively simple adaptation of whole-body PBPK model provide a quantitative estimate of the PK exposures of isoniazid and rifampin in brain

intracellular, relative to brain interstitial fluid.

Our study had several notable limitations. The pharmacogenetic association of SLCO1B1 variability with lower rifampin exposures was based on analysis from two independent clinical studies, and we recognize that heterozygous alleles at additional loci likely relate to rifampin PK variability [43]. In pharmacogenetic studies that were reported subsequent to the work used in our PBPK model development and validation, the rs11045819 allele was found to be rare in certain populations [44]. Linkage disequilibrium analyses, both between- and within-populations, will be essential to improve understanding of the SNPs tags that correspond to gene function [45]. For simplicity, we assigned the drug dose (mg) based on body weight (kg), rather than using dosing bands that allow for fixed-dose combination, and the additional impact of weight-based dosing bands would be of interest in a future study [46]. Furthermore, recent clinical trials have also studied even higher rifampin doses than we selected for simulation purposes, up to 50 mg/kg [47]. Strengths of our approach included the utilization of previously validated PBPK models for each drug, the formal validation of the SLCO1B1 genotype as a novel covariate effect in the rifampin PBPK model, and the additional measurements of MIC distributions for isoniazid and rifampin among *M. tuberculosis* isolates cultured from TBM patients.

In summary, our PBPK-based approach demonstrated that the likelihood of target attainment during TBM treatment is jointly influenced by host pharmacogenetics and pathogen MIC variability. Within a PK-PD framework, the combination of these factors also identifies those patients most likely to benefit from intensified drug therapy. We propose that prospective clinical trials of TBM therapies should routinely capture these determinants of clinical response.

Funding

This study was supported by internal funding.

Transparency declarations

None to declare.

Author contributions statement

KM and CV designed the analyses; KM performed the hands-on analyses and preparation of the first draft of the manuscript; NK and BK performed MIC analysis; All authors were involved in reviews and revisions of the manuscript.

Appendix A. Supplementary data

Supplementary data to this article can be found online at https://doi.org/10.1016/j.tube.2022.102271.

References

[1] Seddon JA, Wilkinson R, van Crevel R, Figaji A, Thwaites GE, Aarnoutse RE, et al. Knowledge gaps and research priorities in tuberculous meningitis. Wellcome Open Res 2019;4:1–18.
[2] Mezochow A, Thakur K, Vinnard C. Tuberculous meningitis in children and adults: new insights for an ancient foe. Curr Neurol Neurosci Rep 2017;17(11).
[3] Nahid P, Dorman SE, Alipanah N, Barry PM, Brozek JL, Cattamanchi A, et al. Executive summary: official American thoracic society/centers for disease control and prevention/infectious diseases society of America clinical practice guidelines: treatment of drug-susceptible tuberculosis. Clin Infect Dis 2016;63(7):853–67.
[4] Heemskerk AD, Bang ND, Mai NTH, Chau TTH, Phu NH, Loc PP, et al. Intensified antituberculosis therapy in adults with tuberculous meningitis. N Engl J Med 2016;374(2):124–34.
[5] Dian S, Yunivita V, Ganiem AR, Pramaesya T, Chaidir L, Wahyudi K, et al. Double-blind, randomized, placebo-controlled phase II dose-finding study to evaluate high-dose rifampin for tuberculous meningitis. Antimicrob Agents Chemother 2018;62(12):1–12.
[6] Cresswell FV, Te Brake L, Atherton R, Ruslami R, Dooley KE, Aarnoutse R, et al. Intensified antibiotic treatment of tuberculosis meningitis. Expet Rev Clin Pharmacol 2019 Mar;12(3):267–88.
[7] Donald PR. Chemotherapy for tuberculous meningitis. N Engl J Med 2016;374(2):179–81. https://doi.org/10.1056/NEJMe1511990. Available from:.
[8] Cox H, Mizrahi V. The coming of age of drug-susceptibility testing for tuberculosis. N Engl J Med 2018;379(15):1474–5.
[9] Gumbo T, Angulo-Barturen I, Ferrer-Bazaga S. Pharmacokinetic-pharmacodynamic and dose-response relationships of antituberculosis drugs: recommendations and standards for industry and academia. J Infect Dis 2015;211(Suppl 3):S96–106.
[10] Naidoo A, Chirehwa M, Ramsuran V, McIlleron H, Naidoo K, Yende-Zuma N, et al. Effects of genetic variability on rifampicin and isoniazid pharmacokinetics in South African patients with recurrent tuberculosis. Pharmacogenomics 2019;20(4):224–40.
[11] Vinnard C, Ravimohan S, Tamuhla N, Ivaturi V, Pasipanodya J, Srivastava S, et al. Isoniazid clearance is impaired among human immunodeficiency virus/tuberculosis patients with high levels of immune activation. Br J Clin Pharmacol 2017;83(4):801–11.
[12] Vinnard C, Ravimohan S, Tamuhla N, Pasipanodya J, Srivastava S, Modongo C, et al. Markers of gut dysfunction do not explain low rifampicin bioavailability in HIV-associated TB. J Antimicrob Chemother 2017;72(7):2020–7.
[13] Weiner M, Peloquin C, Burman W, Luo CC, Engle M, Prihoda TJ, et al. Effects of tuberculosis, race, and human gene SLCO1B1 polymorphisms on rifampin concentrations. Antimicrob Agents Chemother 2010;54(10):4192–200.
[14] Jayaram R, Gaonkar S, Kaur P, Suresh BL, Mahesh BN, Jayashree R, et al. Pharmacokinetics-pharmacodynamics of rifampin in an aerosol infection model of tuberculosis. Antimicrob Agents Chemother 2003;47(7):2118–24.
[15] Gumbo T, Pasipanodya JG, Nuermberger E, Romero K, Hanna D. Correlations between the hollow fiber model of tuberculosis and therapeutic events in tuberculosis patients: learn and confirm. Clin Infect Dis 2015;61(Suppl 1):S18–24.
[16] Vinnard C, King L, Munsiff S, Crossa A, Iwata K, Pasipanodya J, et al. Long-term mortality of patients with tuberculous meningitis in New York city: a cohort study. Clin Infect Dis 2017;64(4):401–7.
[17] Vinnard C, Winston CA, Wileyto EP, Macgregor RR, Bisson GP. Isoniazid resistance and death in patients with tuberculous meningitis: retrospective cohort study. BMJ 2010 Sep;341:c4451.
[18] Woods GL, Brown-Elliott BA, Conville PS, Desmond EP, Hall GS, Lin G, et al. second ed. Wayne (PA: Clinical and Laboratory Standards Institute; 2011 Mar Report No.: M24-A2. [Internet]. Wayne (PA); 2011. Available from: https://www.ncbi.nlm.nih.gov/books/NBK544374/.
[19] Hanke N, Frechen S, Moj D, Britz H, Eissing T, Wendl T, et al. PBPK models for CYP3A4 and P-gp ddi prediction: a modeling network of rifampicin, itraconazole, clarithromycin, midazolam, alfentanil, and digoxin. CPT Pharmacometrics Syst Pharmacol 2018;7(10):647–59.
[20] Rodgers T, Rowland M. Physiologically based pharmacokinetic modelling 2: predicting the tissue distribution of acids, very weak bases, neutrals and zwitterions. J Pharm Sci 2006 Jun;95(6):1238–57.
[21] Cordes H, Thiel C, Aschmann HE, Baier V, Blank LM, Kuepfer L. A physiologically based pharmacokinetic model of isoniazid and its application in individualizing tuberculosis chemotherapy. Antimicrob Agents Chemother 2016;60(10):6134–45.
[22] Lippert J, Burghaus R, Edginton A, Frechen S, Karlsson M, Kovar A, et al. Open systems Pharmacology community—an open access, open source, open science approach to modeling and simulation in pharmaceutical sciences. CPT Pharmacometrics Syst Pharmacol 2019;8(12):878–82.
[23] Cresswell FV, Meya DB, Kagimu E, Grint D, Te Brake L, Kasibante J, et al. High-dose oral and intravenous rifampicin for the treatment of tuberculous meningitis in predominantly human immunodeficiency virus (HIV)-Positive Ugandan adults: a phase II open-label randomized controlled trial. Clin Infect Dis 2021;73(5):876–84.
[24] Kaojarern S, Supmonchai K, Phuapradit P, Mokkhavesa C, sarinee Krittiyanunt. Effect of steroids on CSF penetration of antituberculous drugs in tuberculous meningitis. Clin Pharmacol Ther 1991;49(1):6–12.
[25] Brown TS, Narechania A, Walker JR, Planet PJ, Bifani PJ, Kolokotronis SO, et al. Genomic epidemiology of Lineage 4 Mycobacterium tuberculosis subpopulations in New York city and New Jersey, 1999-2009. BMC Genom 2016;17(1):1–11. https://doi.org/10.1186/s12864-016-3298-6. Available from:.
[26] Woods GL, Brown-Elliott BA, Conville PS, Desmond EP, Hall GS, Lin G, et al. Susceptibility testing of mycobacteria, nocardiae, and other aerobic actinomycetes. second ed. Wayne (PA): Clinical and Laboratory Standards Institute; 2011.
[27] Rajman I, Knapp L, Hanna I. Genetic diversity in drug transporters: impact in african populations. Clin Transl Sci 2020 Sep;13(5):848–60.
[28] Gumbo T, Louie A, Liu W, Brown D, Ambrose PG, Bhavnani SM, et al. Isoniazid bactericidal activity and resistance emergence: integrating pharmacodynamics and pharmacogenomics to predict efficacy in different ethnic populations. Antimicrob Agents Chemother 2007;51(7):2329–36.
[29] Boeree MJ, Diacon AH, Dawson R, Narunsky K, Du Bois J, Venter A, et al. A dose-ranging trial to optimize the dose of rifampin in the treatment of tuberculosis. Am J Respir Crit Care Med 2015;191(9):1058–65.
[30] Davis A, Meintjes G, Wilkinson RJ. Treatment of tuberculous meningitis and its complications in adults. Curr Treat Options Neurol 2018;20(3).
[31] Nau R, Djukic M, Spreer A, Eiffert H. Bacterial meningitis: new therapeutic approaches. Expert Rev Anti Infect Ther 2013;11(10):1079–95. https://doi.org/10.1586/14787210.2013.839381. Available from:.
[32] Ruslami R, Gafar F, Yunivita V, Parwati I, Ganiem AR, Aarnoutse RE, et al. Pharmacokinetics and safety/tolerability of isoniazid, rifampicin and pyrazinamide in children and adolescents treated for tuberculous meningitis. Arch Dis Child 2021:70–7.

[33] Svensson EM, Dian S, Te Brake L, Ganiem AR, Yunivita V, Van Laarhoven A, et al. Model-based meta-analysis of rifampicin exposure and mortality in Indonesian tuberculous meningitis trials. Clin Infect Dis 2020;71(8):1817–23.
[34] Ding J, Thuy Thuong Thuong N, Pham T Van, Heemskerk D, Pouplin T, Tran CTH, et al. Pharmacokinetics and pharmacodynamics of intensive antituberculosis treatment of tuberculous meningitis. Clin Pharmacol Ther 2020;107(4):1023–33.
[35] Velásquez GE, Brooks MB, Coit JM, Pertinez H, Vásquez DV, Garavito ES, et al. Efficacy and safety of high-dose rifampin in pulmonary tuberculosis a randomized controlled trial. Am J Respir Crit Care Med 2018;198(5):657–66.
[36] Gliddon HD, Frampton D, Munsamy V, Heaney J, Pataillot-Meakin T, Nastouli E, et al. A rapid drug resistance genotyping workflow for Mycobacterium tuberculosis, using targeted isothermal amplification and nanopore sequencing. Microbiol Spectr 2021;9(3):1–12.
[37] van Crevel R, Avila-Pacheco J, Thuong NTT, Ganiem AR, Imran D, Hamers RL, et al. Improving host-directed therapy for tuberculous meningitis by linking clinical and multi-omics data. Tuberculosis 2021;128:102085. Available from: https://www.sciencedirect.com/science/article/pii/S1472979221000354.
[38] Donovan J, Phu NH, Thao LTP, Lan NH, Mai NTH, Trang NTM, et al. Adjunctive dexamethasone for the treatment of hiv-uninfected adults with tuberculous meningitis stratified by leukotriene a4 hydrolase genotype (LAST ACT): study protocol for a randomised double blind placebo controlled non-inferiority trial [version 1; r. Wellcome Open Res 2018;3:1–19.
[39] Donald PR, Schaaf HS, Schoeman JF. Tuberculous meningitis and miliary tuberculosis: the Rich focus revisited. J Infect 2005 Apr;50(3):193–5.
[40] Rock RB, Olin M, Baker CA, Molitor TW, Peterson PK. Central nervous system tuberculosis: pathogenesis and clinical aspects. Clin Microbiol Rev 2008;21(2):243–61.
[41] Singh AK, Malhotra HS, Garg RK, Jain A, Kumar N, Kohli N, et al. Paradoxical reaction in tuberculous meningitis: presentation, predictors and impact on prognosis. BMC Infect Dis 2016;16(1):1–11. https://doi.org/10.1186/s12879-016-1625-9. Available from:.
[42] Thiel C, Schneckener S, Krauss M, Ghallab A, Hofmann U, Kanacher T, et al. A systematic evaluation of the use of physiologically based pharmacokinetic modeling for cross-species extrapolation. J Pharm Sci 2015 Jan;104(1):191–206.
[43] Thomas L, Miraj SS, Surulivelrajan M, Varma M, Sanju CSV, Rao M. Influence of single nucleotide polymorphisms on rifampin pharmacokinetics in tuberculosis patients. Antibiotics 2020;9(6):1–15.
[44] Sloan DJ, McCallum AD, Schipani A, Egan D, Mwandumba HC, Ward SA, et al. Genetic determinants of the pharmacokinetic variability of rifampin in Malawian adults with pulmonary tuberculosis. Antimicrob Agents Chemother 2017;61(7):1–9.
[45] Tishkoff SA, Reed FA, Friedlaender FR, Ehret C, Ranciaro A, Froment A, et al. The genetic structure and history of Africans and African Americans. 80 Science 2009;324(5930):1035–44.
[46] Sekaggya-Wiltshire C, Chirehwa M, Musaazi J, Von Braun A, Buzibye A, Muller D, et al. Low antituberculosis drug concentrations in HIV-tuberculosis-coinfected adults with low body weight: is it time to update dosing guidelines? Antimicrob Agents Chemother 2019;63(6):1–11.
[47] Wasserman S, Davis A, Stek C, Chirehwa M, Botha S, Daroowala R, et al. Plasma pharmacokinetics of high-dose oral versus intravenous rifampicin in patients with tuberculous meningitis: a randomized controlled trial. Antimicrob Agents Chemother 2021;65(8).